Journal of Chromatography A 1701 (2023) 464051

Contents lists available at ScienceDirect

Journal of Chromatography A

journal homepage: www.elsevier.com/locate/chroma

Two-dimensional separation of water-soluble polymers using size exclusion and reversed phase chromatography employing capillary-channeled polymer fiber columns ☆

Sarah K. Wysor, R. Kenneth Marcus*

Department of Chemistry, Biosystems Research Complex, Clemson University, Clemson, SC 29634-0973, USA

ARTICLE INFO

Article history:
Received 14 March 2023
Revised 3 May 2023
Accepted 4 May 2023
Available online 8 May 2023

Keywords:
Two-dimensional liquid chromatography (2DLC)
Water-soluble polymers
Capillary channeled polymer fiber
Size exclusion chromatography
Reversed phase chromatography

ABSTRACT

Polymeric materials are readily available, durable materials that have piqued the interest of many diverse fields, ranging from biomedical engineering to construction. The physiochemical properties of a polymer dictate the behavior and function, where large polydispersity among polymer properties can lead to problems; however, current polymer analysis methods often only report results for one particular property. Two-dimensional liquid chromatography (2DLC) applications have become increasingly popular due to the ability to implement two chromatographic modalities in one platform, meaning the ability to simultaneously address multiple physiochemical aspects of a polymer sample, such as functional group content and molar mass. The work presented employs size exclusion chromatography (SEC) and reversed-phase (RP) chromatography, through two coupling strategies: SEC x RP and RP x RP separations of the water-soluble polymers poly(methacrylic acid) (PMA) and polystyrene sulfonic acid (PSSA). Capillary-channeled polymer (C-CP) fiber (polyester and polypropylene) stationary phases were used for the RP separations. Particularly attractive is the fact that they are easily implemented as the second dimension in 2DLC workflows due to their low backpressure (<1000 psi at ~70 mm sec^{-1}) and fast separation times. In-line multi-angle light scattering (MALS) was also implemented for molecular weight determinations of the polymer samples, with the molecular weight of PMA ranging from 5×10^4 to 2×10^5 g mol^{-1}, while PSSA ranges from 10^5 to 10^8 g mol^{-1}. While the orthogonal pairing of SEC x RP addresses polymer sizing and chemistry, this approach is limited by long separation times (80 min), the need for high solute concentrations (PMA = 1.79 mg mL^{-1} and PSSA = 0.175 mg mL^{-1} to yield comparable absorbance responses) due to on-column dilution and subsequently limited resolution in the RP separation space. With RP x RP couplings, separation times were significantly reduced (40 min), with lower sample concentrations (0.595 mg mL^{-1} of PMA and 0.05 mg mL^{-1} of PSSA) required. The combined RP strategy provided better overall distinction in the chemical distribution of the polymers, yielding 7 distict species versus 3 for the SEC x RP coupling.

1. Introduction

Polymers are implemented across many fields, ranging from everyday plastics to bioprosthetics and construction materials [1–4]. The physiochemical properties of a polymer are primarily linked to its chemical functionality and molecular weight; therefore, it is essential to control the chemical and physical makeup of a polymer to successfully realize its intended use. Synthetic and natural polymers are usually comprised of multicomponent mixtures, each contributing to the various structural and functional features that are present within the bulk polymer. Such physiochemical features can include unwanted variations in molar mass, chemical composition, functionality, and molecular topology [5]. For instance, the molecular weight of a polymer is linked to its mechanical properties, and even pure polymers will have some naturally-present polydispersity [6]. The analysis of polymers is often performed using light scattering, NMR, and end group titrations to characterize average polymer properties, such as chain length, chemical functionality, etc. [7,8]. Still, these methods only provide the average properties of polymers, meaning very little information about the

Abbreviations: 2DLC, Two-dimensional liquid chromatography; C-CP, Capillary channeled polymer; MALS, Multiangle light scattering; PET, Polyester; PMA, Poly(methacrylic acid); PP, Polypropylene; PSSA, Polystyrene sulfonic acid; RP, Reversed phase; SEC, Size exclusion chromatography.

☆ Submitted for publication in the Special Issue on Advances in Multidimensional Chromatography in the Journal of Chromatography A

* Corresponding author.
E-mail address: marcusr@clemson.edu (R.K. Marcus).

https://doi.org/10.1016/j.chroma.2023.464051
0021-9673/

property distributions present within the polymer sample is provided [5].

The chromatographic separation of polymers has proven to be beneficial in determining the composite heterogeneity of the monomers regarding the size and chemical attributes, with common separations including size exclusion chromatography (SEC) [9–11] and reversed-phase chromatography (RP) [12–14]. For both of these modalities, single-dimension HPLC separations are limited to characterizing only a single chemical or physical property of a polymer. A multitude of SEC separations of polymers have been performed [15–19], where these isolations are very easy to implement as they are based on no chemical interaction, require little to no sample preparation, and use chemically-simple mobile phases. However, with SEC, solutes are eluted based on their hydrodynamic volume, while polymers also often display multiple distributions in their physical and chemical properties simultaneously [5]. With SEC, co-elution problems can occur, leading to inaccurate conclusions regarding the size or molecular weight of the analyte. For example, conformation changes such as a globular analyte relaxing to a rod-like conformation would cause a faster elution, which could be interpreted as a higher molecular weight. With the sensitive nature of polymers to pH, solvent composition, temperature, etc., contributing to conformation changes [20], SEC applied alone can be problematic. Due to the possibility of misinterpretation, SEC requires additional steps for the confirmation of sizing and molecular weight, such as multi-angle light scattering (MALS), which provides the sensitive comprehensive distribution of the molecular weight of the polymer without the need for calibration standards.

RP separations have ample benefits because of their wide applicability, fast equilibrium, high efficiency, differences in selectivity, and compatibility with mass spectrometry (MS) [21]. Gradients are also used to improve peak capacity while eliminating carry-over effects and providing better band compression effects, meaning narrow peaks [22]. Previous efforts by Marcus et al. have shown water-soluble polymer separations through RP chromatography when SEC was not an option due to similarities in the hydrodynamic radii of the polymers [13]. However, this separation modality still only reveals the chemical distribution, and coelution problems can occur with species of similar chemistries. Polymers often exhibit variations in chemical structures based on RP solvent composition, such as linear/branched chains or differing end/functional groups. As such, RP separations have proven successful in isolating these sorts of chemical composition distributions [12,14,23,24]. However, RP separations of polymers can also present challenges. For instance, with complex polymer samples, or when large polydispersity is present within a polymer population, coelution can occur, yielding poor resolution. Overall, with traditional single-dimensional chromatography, regardless of the modality, polymer analysis is limited to only addressing a single physical or chemical attribute.

Two-dimensional liquid chromatography (2DLC) offers improved peak capacities (the ability to separate peaks) for complex species by incorporating two separation modalities within a single platform [25–27]. Ideally, the peak capacity of 2DLC is determined by the product of the peak capacity of each dimension as described by Giddings [28]. To realize the increased peak capacity attainable by using 2DLC, orthogonal separation modalities must be used in the respective dimensions [29–31]. When orthogonal methods are coupled, there is more “separation space”, referring to the area for the peaks to separate in two-dimensional space [32,33]. Therefore, separations with higher levels of orthogonality often yield improved resolution and peak capacity. 2DLC can be used for characterizing diverse forms of heterogeneity within polymers because this technique can separate the physical and chemical property distributions in a given sample through the use of commonly implemented separation modalities, such as SEC and RP [34,35]. The addition of a second dimension provides the selectivity and resolution to address two properties in a given polymer population simultaneously [36]. Implementation of this technique offers opportunities for a more comprehensive analysis of polymers, specifically enabling information about polymer physiochemical heterogeneity to be obtained.

As there is an immense variety of polymers of different chemistries, posing the challenge to characterize them based on their makeup. As such, there continues to be a drive to achieve more efficient column formats for 1D and 2D separations. To this end, Marcus and co-workers have developed capillary-channeled polymer (C-CP) fiber stationary phases based on polypropylene (PP), polyethylene terephthalate (PET), and nylon base polymers [37,38]. Fortuitously, the lack of substrate porosity (and therefore low phase ratios) makes the fibers poor candidates for *small molecule* applications [37,39], but optimal for applications in macromolecule (protein and polymer) separations as there is no intraphase diffusion (and therefore no van Deemter C-term effects) [40–42]. Additionally, the C-CP base polymers provide the opportunity for surface modifications, to affect cation exchange [43,44], anion exchange [45], and affinity [46–49] columns. C-CP fibers self-align when packed into columns, creating multiple interdigitating parallel channels that create efficient mass transfer characteristics, allowing them to be used at high linear velocities with little peak broadening and low backpressures ($<$1000 psi at $\sim$70 mm sec^{-1}) [41,50]. The reduced backpressures of the C-CP fibers eliminate the need for expensive ultrahigh-pressure pumps in the second dimension (^{2}D), while providing fast separation times [51]. Additionally, previous studies have evaluated the performance of RP separations using C-CP fiber columns to commercial columns [52], determining that the C-CP columns were more sutiable and efficient when implemented in the second dimension due to the ease of re-equilibrating in the fast cycling times [51].

In this study, trilobal polypropylene (PP) and 8-channeled polyethylene terephthalate (PET) fibers were used as the stationary phases for the RP separations of water soluble polymers, poly(methacrylic acid) (PMA) and polystyrene sulfonic acid (PSSA). The monomeric structures of the two fiber types and polymer solutes are presented in Fig. 1. Both fiber types have been demonstrated to effectively separate proteins using more or less standard reversed phase gradients, where increasing organic content elutes the solutes based on their relative hydrophobicity [40,50,53]. The PP and PET fibers offer different levels of hydrophobicity and types of solute-surface interactions because of the differences in polymer chemistries; PP being solely aliphatic in nature and the PET surface including aromatic and polar carbonyl functional groups. In addition, the end groups of PET are anionic carboxylic acids. Thus solute retention on the PET phase likely entails aspects of electrostatic interactions as well as hydrophobicity. Both fiber types were employed previously in the 1D separations of water soluble polymers [13]. A key aspect of the C-CP fiber phases is a complete lack of size-exclusion phenomena below molecular weights of $\sim$2000 Da . Thus the separations are completely enthalpic in nature [52,54,55]. In terms of the solutes, PMA contains a carboxylic acid group as the primary functional group while PSSA contains an aromatic ring and a sulfonic acid group. Beyond the comparatively benign PP surface, the expected interactions between the solutes and PET surfaces for the RP separations include pi-pi interactions between the aromatic rings, hydrogen bonding with carbonyl groups, and hydrophobic interactions with the ethylene unit present in the fiber.

This study will examine two 2DLC separation approaches, comparing SEC $\times$ RP and RP $\times$ RP methods for the separation of the two water-soluble polymers, PMA and PSSA. In the first case, separations based on hydrodynamic radii are followed by

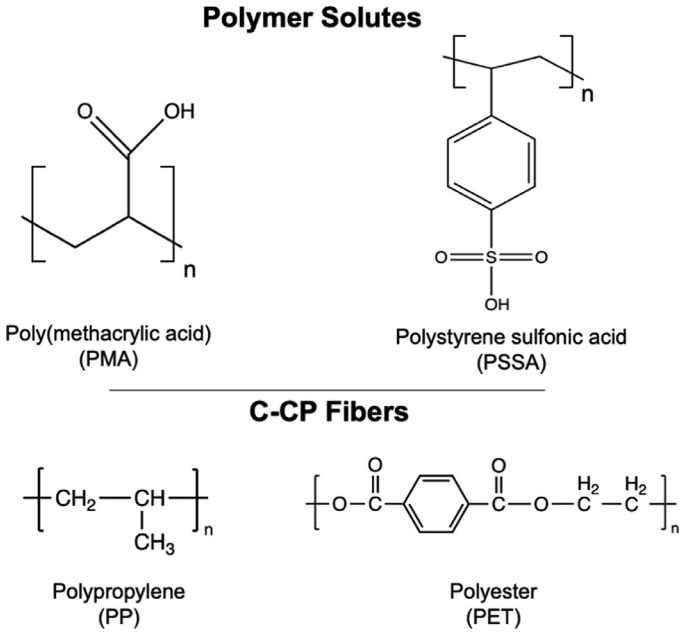

Fig. 1. Structures of the polymer solutes poly(methacrylic acid) (PMA) and polystyrene sulfonic acid (PSSA), and the C-CP fiber stationary phases polypropylene (PP) and polyethylene terephthalate (PET).

hydrophobicity-based (at least nominally) isolation on the two fiber types. In the latter case, hydrophobicity is the primary means of separation, but on two different phases in two couplings; PET × PP and PP × PET C-CP fibers. Molecular weights were determined following SEC with in-line MALS for each polymer as a confirmation for the characterization. The results presented here demonstrate the efficacy of the C-CP fiber phase as an efficient, effective stationary phase in the 2D separations of water soluble polymers.

2. Materials and methods

2.1. Chemicals and sample preparation

HPLC-grade acetonitrile (ACN) (VWR Chemical, Radnor, PA), deionized water (DI-H_2O) from an Elga PURELAB flex water purification system (18.2 MΩ cm−1) (Veolia Water Technologies, High Wycombe, England), and trifluoroacetic acid (TFA) (Sigma-Aldrich, Milwaukee, WI, USA) were used for sample and mobile phase preparation. Poly(methacrylic acid) (PMA) (Polysciences, Inc., Warrington, PA, USA) with an average molecular weight ∼100,000 and polystyrene sulfonic acid (PSSA) (Scientific Polymer Products, Inc., Ontario, New York, USA) with an average molecular weight ∼70,000 (presented as 20% solids/mixture in water), were used as the analytes and diluted accordingly the day of the experiment.

2.2. Chromatographic columns

As previously described, the PET and PP C-CP fibers were manufactured by the Department of Material Science and Engineering at Clemson University [56]. Briefly, the PET and PP fibers were pulled through polyether ether ketone (PEEK) tubing (0.76 mm inner diameter) and cut to a 30 cm column length. The number of fibers of each was chosen to achieve an interstitial fraction of ∼0.6. Upon packing, the fiber columns were washed with DI-H_2O, ACN, then DI-H_2O again until stable absorbance baselines were achieved at 224 nm. An X-Bridge BEH SEC Column, 200 Å, 3.5 μm, 7.8 mm X 300 mm (Waters, Milford, MA, USA) with ethylene hybrid particle technology with a diol-bonded surface was used for size exclusion (SEC) separations, with an ideal separation range falling between 10,000 and 450,000 Da.

2.3. Instrumentation

Chromatographic measurements were performed using an Agilent 2D HPLC (Agilent Technologies, Santa Clara, CA) equipped with the ^{1}D: 1260 binary pump, 1260 degasser, 1100 multiple wavelength detector; 1290 valve drive; ^{2}D: 1290 UHPLC high-speed pump, and 1290 variable wavelength detector. (While provided in this commercial package, it must be clearly stated that operation with C-CP fiber columns in ^{2}D does not require the backpressure capacities of a UPLC pump.) ChemStation software and OpenLab was used to operate the 2DLC instrumentation. A UV detection wavelength of 224 nm was used for the entirety of this study due to the strong optical absorbance of both polymer solutes at this wavelength. All product chromatograms are plotted following an absorbance background correction through the coarse of the separations based on the injection of a solvent blank. Two-dimensional chromatograms were processed in GC x GC Images followed by Origin (OriginLab Corp., Northampton, MA), whose output is in the form of heat maps. The absolute values of the color scales is not comparable between chromatograms due to the differences in background correction. MALS measurements were performed following SEC separations on the DAWN MALS detector (Wyatt, Santa Barbara, CA, USA), controlled via ASTRA software. The flow cell cuvette, surrounded by 18 photodetectors, was placed in-line with the Agilent 2DLC, following the ^{1}D column exit. The dn/dc values (required for proper calibration) for PMA and PSSA were 0.175 and 0.17, respectively, provided through the Wyatt database.

2.4. Chromatographic methods

2.4.1. ^{1}D SEC and RP

Mobile phases for both dimensions consisted of 100% DI-H_2O + 0.1% TFA as mobile phase A (MP A) and 100% ACN + 0.1% TFA as mobile phase B (MP B). Before coupling, standalone SEC and RP separations were performed with the individual columns. For SEC, isocratic separations were performed at a flow rate of 0.5 mL min^{-1}, with mobile phase B compositions evaluated across a range of 0 – 30%, in an effort to minimize adsorption to the SEC stationary phase. Analyte injection volumes of 20 µL were employed with the respective solute concentrations (PMA = 1.79 mg mL^{-1} and PSSA = 0.175 mg mL^{-1}) chosen to affect comparable absorbance responses. Importantly, both of these values are far below the solutes' respective solubility limits. A 100% ACN wash followed the SEC separation to ascertain if any polymer solute had adsorbed onto the SEC phase. Initially, for RP separation, a linear gradient from 0 to 100% MP B was performed on each C-CP fiber column type at flow rates of 0.5 mL min^{-1}, followed by the use of step gradients programs. For the PET, a step gradient consisted of: 0%B (0 – 1 min), 0 – 30% (1 – 2 min), held at 30%B (3 – 4 min), 30 – 50% MP B (4 – 5 min), and finally held at 50% B (5 – 6 min), while for PP: 0% B (0 – 1 min), 0 – 20%B (1 – 2 min), held at 20%B (2 – 3 min), 20 – 50%B (3 – 4 min), and held at 50%B (4 – 5 min).

2.4.2. SEC x RP

For the coupled SEC x RP separations, ^{1}D separations were performed at a flow rate of 0.1 mL min^{-1} on the X-Bridge SEC column due to the low flow rate required for the ^{1}D eluate transfer to ^{2}D. PP and PET columns were used as the RP phases in the ^{2}D separations. The solvent gradients were optimized using the results of the standalone (1D) separations and then translated into ^{2}D. The flow rate was varied between 0.5 – 0.7 mL min^{-1}, and

gradient times (0–50% B) were varied between 30 and 42 s to determine optimal separation conditions. In each case, the column re-equilibration (re-set) time between gradients was 6 s. All chromatographic data were collected in triplicate, with absorbance values background subtracted based on DI-H_2O injections to match the gradients of the analyses.

2.4.2. RP x RP

It is important to understand that the two C-CP fiber phases have different chemistries. PP is very hydrophobic with no ionizable functional groups, while PET is less hydrophobic with anionic carboxylate end groups present at neutral pH. Mobile phases were maintained as listed above for the reversed phase coupled separations. For RP separations, a 20 µL injection volume composed of 0.595 mg mL^{-1} of PMA and 0.05 mg mL^{-1} of PSSA was used to achieve comparable absorbance responses for the solutes. The two C-CP fiber stationary phases were employed in different orders; PP x PET and PET x PP. When coupling PP x PET, the ^{1}D PP separation consisted of a linear gradient from 0 to 50% MP B at 0.1 mL min^{-1} for 40 min, while the PET ^{2}D consisted of a shift gradient, where the starting solvent composition increases with each successive ^{2}D injection, was used in the ^{2}D to reduce the optical absorbance background of the separations due to better mobile phase composition matches in the eluate transfer. Shift gradients were used for all RP x RP separations, with flow rates varied as before from 0.5 to 0.7 mL min^{-1}, and separation times from 36 to 48 s. For PET x PP arrangement, the PET ^{1}D gradient was the same as above, while also using a shift gradient at the same varied flow rates and separation times as listed above. Critical in the consideration of using the C-CP fibers in 2D is the fact that high linear velocities of 50 mm s^{-1} are achieved at backpressures of 300–400 psi, negating the need for UPLC pumping capacities in the second dimension. Chromatographic data were collected in triplicate ($n = 3$), with the optical background subtracted with DI-H_2O injections.

3. Results and discussion

3.1. 1D separations

The target operation qualities for the ^{1}D and ^{2}D portions of 2DLC separations are quite different. The general concepts have been presented in detail in a number of excellent papers [26,57–60]. Simply, in ^{1}D, the primary goal is the introduction of narrow, well-resolved bands to the ^{2}D injection port. Narrow bands are desirable to allow for the fewest number, of highly concentrated injections into the second stage. High resolution is also desired to minimize potential wraparound in the ^{2}D; i.e., allow sufficient time to affect the ^{2}D separation before the next component elutes from the first stage. The critical metric in ^{2}D is the resolution of components within each fraction injected, but on time scales that allow for rapid injection of subsequent ^{1}D bands. In this regard, rapid gradient programs with minimal need for column re-equilibration are desired. The following sections describe the optimization of these characteristics for each column/elution combination, performed as 1D experiments to project their ^{1}D implementation. While not completely conclusive, such efforts provide an effective approach prior to adding to the complexity of multiple dimensions.

3.1.1. SEC separations

With SEC separations, interactions between the stationary phase and analyte are undesirable, as the separation is entropy-driven, where an analyte's elution characteristics (e.g., time and bandwidth) are dependent on the solute's hydrodynamic volume. To this end, hydrophobic interactions between the solutes and the stationary phase material must be minimized. Various percentages (0–30%) of the acetonitrile (ACN) were used to determine the optimal SEC conditions for the separation, based on the band elution characteristics. Following each SEC cycle, a 100% ACN wash was used to determine if polymers had adsorbed to the SEC column. The respective chromatograms are presented in Fig. 2 for single-solute and mixture injections. For a mobile phase consisting of no (0%) ACN (Fig. 2a), the PMA component separation showed little to no elution, indicating PMA adsorption onto the column, while the PSSA elution displays two distinct peaks, indicating two different size ranges of the polymer. Very interestingly, the polymer mixture eluted at 0% ACN exhibited a much higher absorbance for the higher molecular weight (excluded) fraction of the PSSA, with an additional peak appearing around 10 min. Both of these responses suggest an interaction between the two polymers, which may also cause the PMA polymer to elute, rather than retain to the column. The overall peak area for the eluted polymer mixture was ~296 mAu x min, but when comparing the mixture to the individual injections, the PMA and PSSA individual injections only account for ~ 11.3% and 34.9% of the mixture, respectively. The ~53.8% retention could be attributed to electrostatic or hydrophobic interactions occurring between the polymer and the stationary phase, which have been previously reported [61]. To reduce the interactions between the analytes and stationary phase (and perhaps each other), organic modifiers can be incorporated into the mobile phase.

When a 10% ACN modifier was present in the MP (Fig. 2b), the PSSA and PMA each exhibited two peaks, indicating two size regimes for each of the polymers; however, with an apparent coelution window at approximately 12 min. Likewise, a second fraction of the PMA is seen to elute at ~16 min, which was not present in the 0% ACN case, reflective of enthalpic absorption occurring with this small amount of modifier, further seen is a high absorbance response for the 100% can flush. For the elution of the mixture, the absorbance value increased again at the time of the initial eluting band, as seen in the previous case for PSSA. In this instance, there was a slight increase in the peak area of the mixture at 299 mAu x min in comparison to the separation with no ACN, with PMA and PSSA individual injections making up only 17.5% and 30.7% of the mixture, respectively. Again the elution of the mixture shows over a 50% increase in the recovery of the polymer.

At an MP containing 20% ACN (Fig. 2c), each of the individual polymers shows pronounced changes in their elution characteristics in comparison to 10% ACN. In the case of PSSA, the two bands, which had signs of multiple populations, further evolved into having a structural continuum between them. The PMA showed a pronounced change as the initial band occurring at ~12 min is clearly reduced in response, while a new band appears at ~5 min, coincident with the elution time of what has been the most intense band in each of the chromatograms of the pure PSSA and the mixture. At this modifier concentration, the band previously seen at ~16 min disappeared. The new high molecular weight band may represent a fraction that was retained on the column at low ACN concentrations. In addition, the second PMA band at ~16 min shows a shortening in retention time, down to ~13 min. In the case of the mixture injection, the chromatogram is composed of an initial peak at ~5 min, composed of both solutes, a broad feature between 8 and 11 min that is reflective of PSSA, a peak at ~12 min composed primarily of PSSA, and finally, the low mass PMA fraction eluting at ~13 min. In the case of the 20% ACN MP, the chromatogram mixture begins to better-reflect a linear combination of the individual components, though again, with a far greater optical absorbance response at the initial band elution time, seemingly reflecting some, albeit reduced, level of interaction of the two polymers. Finally, under these conditions, the absorbance response to the 100% ACN flush again revealed polymer interactions with the

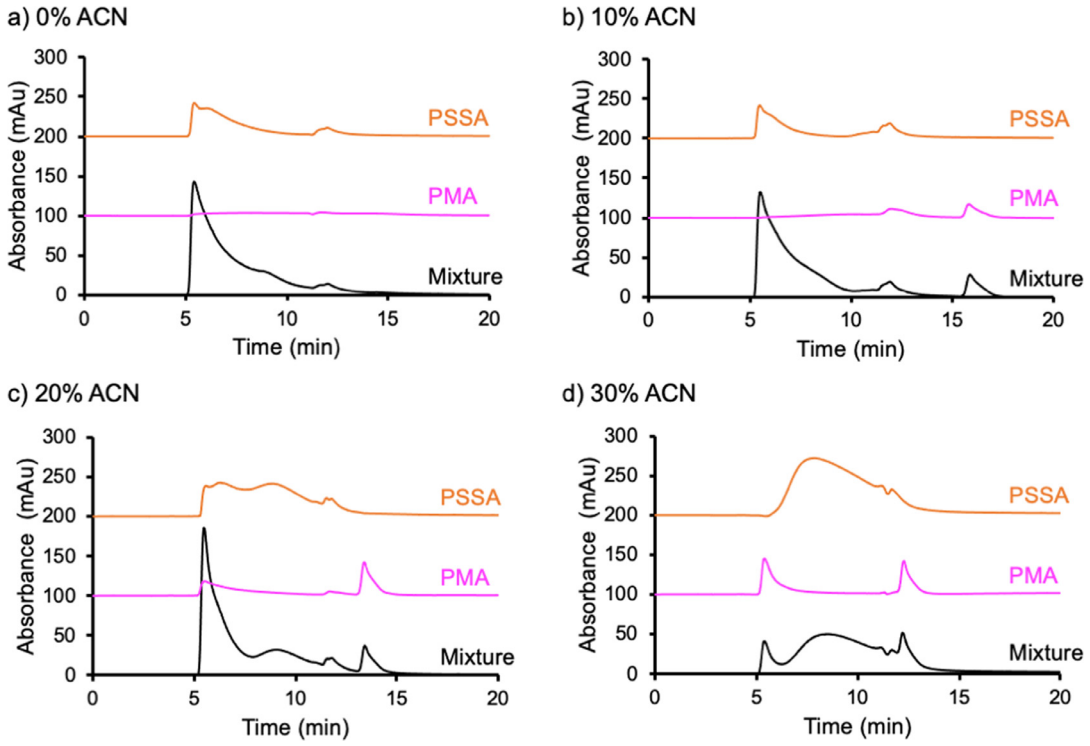

Fig. 2. Size exclusion separation of individual, PMA (pink) and PSSA (orange), and polymer mixtures (black) at varying percentages of ACN + 0.1% TFA in DI + 0.1% TFA is shown. Percentages of ACN included: (a) 0% ACN, (b) 10% ACN, (c) 20% ACN, and (d) 30% ACN. Separations were performed at a flow rate of 0.5 mL min^{-1}.

column, however far less than the 10% ACN separation. Again, the peak area of the mixture increased with the increase in ACN percentage, with an area of 313 mAu x min and PMA and PSSA individual injections representing ~23% and ~70%, respectively, or ~93% of the mixture.

Finally, at an MP concentration of 30% ACN (Fig. 2d), the PSSA is seen to elute as one broad band over a 10 min period, indicating a large range in hydrodynamic volumes and more dispersity in the polymer. This broad peak could result from a distribution in the differing degrees of sulfonation present in the PSSA polymer, which will result in differing degrees of hydrophilicity within the polymer [62] and as unsulfonated styrenes are known to aggregate [63,64]. Here, the PMA elutes in two distinct peaks, likely representing the rod-like and spherical conformations of PMA commonly observed [65–69]. The separation of the mixture shows minimal overlap, along with no polymer interaction with on-column with a peak area of 377 mAu x min. When comparing the mixture to the individual injections, PMA makes up ~17%, and PSSA is ~84%, confirming the complete elution of the polymers in both individual and mixtures. The 30% ACN condition was used as the final SEC condition for the 2DLC separation, keeping in mind that, depending on the specific application, it may not be totally reflective of the desired information. Percentages of ACN higher than 30% were not considered because at percentages above 40%, the polymers would not be retained to the RP ^{2}D column. Based on the SEC separation with 30% ACN, PMA has two distinct hydrodynamic volumes within the sample, while PSSA exhibits a large polydispersed population eluting over about 10 min at a flow rate of 0.5 mL min^{-1}.

In order to confirm the molecular weights of each polymer, as SEC only distinguishes between hydrodynamic volumes, multi-angle light scattering (MALS) was coupled in-line with the SEC column. The addition of in-line MALS allows for the sizing determination based on the scattered light of the analyte, potentially eliminating the need for a calibration curve of molecular weights for the SEC separation. The in-line sizing is especially important for the polymers as they can be found in different conformations, particularly PMA, which is known to have multiple conformations [65–69] as well as potential agglomerates. The molecular weight "chromatograms" for the individual polymers were determined in 30% ACN + 0.1% TFA and are shown in Fig. 3. In both instances, the log molecular mass responses nicely overlap with the absorbance traces. In the case of PMA (Fig. 3a), two fractions are seen, the first covering an absolute size range of 5×10^4 – 2×10^5 g mol^{-1} and the second being a fairly uniform distribution around 6×10^4 g mol^{-1}. For PSSA (Fig. 3b), a very different case is seen, with a very broad range of sizes detected across the elution band, along with evidence of somewhat discrete populations. Here a variation in molar mass is observed over 3 orders of magnitude (10^8 – 10^5 g mol^{-1}) across the PSSA absorbance band. The large discrepancies in molecular weights are likely due to aggregation within the polymer, reflecting the degrees of sulfonation, including some unsulfonated styrene, which is known to occur under these condition [63,64]. In general, the absorbance-based SEC chromatograms seem to be a realistic reflection of the molecular weight distributions of the two polymer in the 30% ACN solvent environment.

3.1.2. RP separations

For the initial evaluation of the C-CP fiber columns, the polymers were separated in standalone (1D) RP separations to determine the relevant elution conditions. Initially, a 0 – 100% linear gradient was performed for the individual polymers and mixtures on the PET and PP fiber columns, as shown in Fig. 4. The linear gradient, RP separation using the PET fiber column (Fig. 4a) exhibited an elution order for the individual polymers of PSSA eluting at ~2.1 min and PMA eluting ~3.1 min. As PET is less hydrophobic than PP (Fig. 4b), the elution time would be expected to be shorter (lower %B for elution); however, this is not the case. PSSA eluted similarly from both the PP and PET fiber phases, while

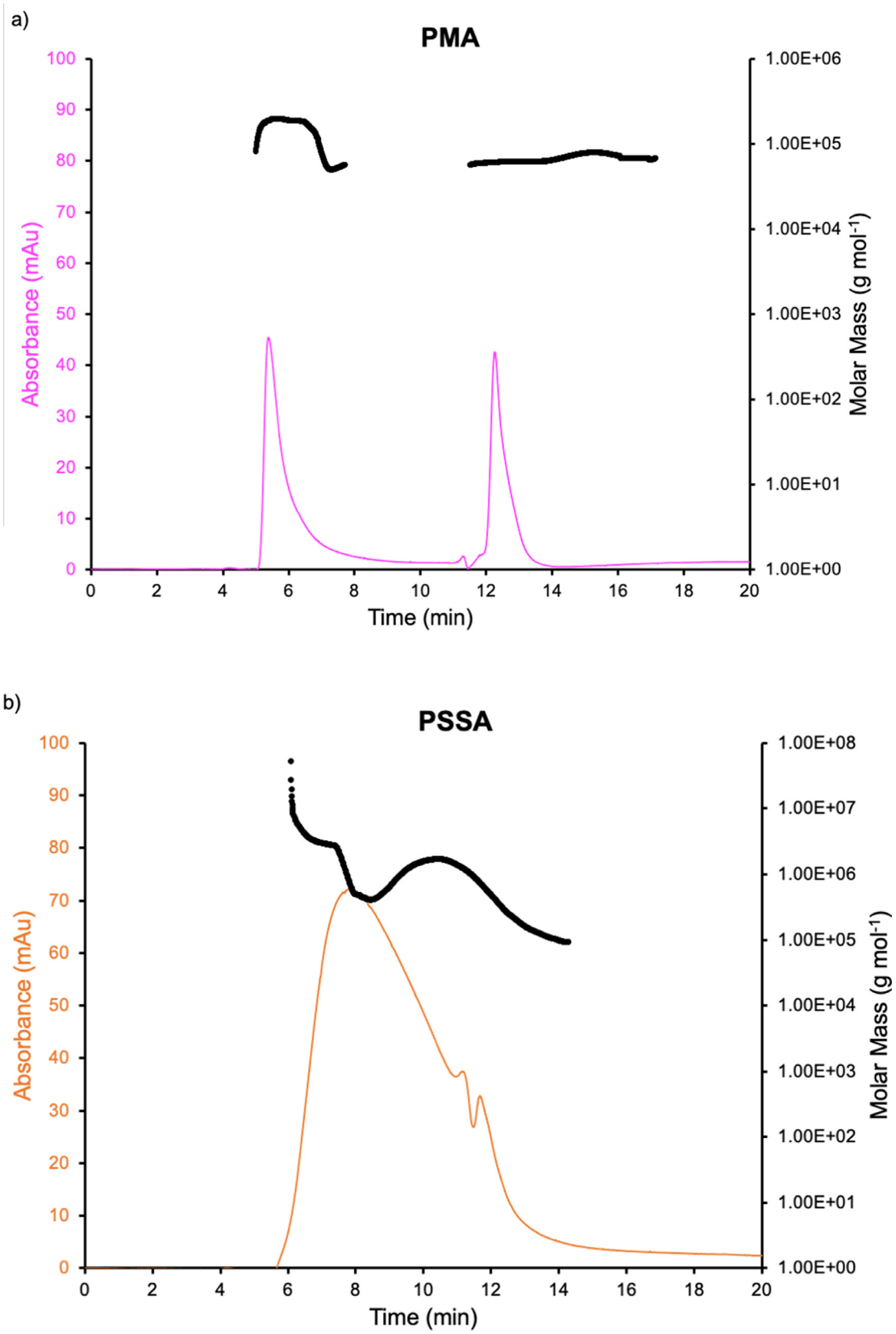

Fig. 3. Molar mass of (a) PMA and (b) PSSA determined via MALS. The MALS was placed in-line with the ^{1}D detector to determine each molar mass of the polymers following the SEC separation at a flow rate of 0.5 mL min^{-1}. The absorbance at 224 nm is plotted on the left y-axis, while the molar mass is plotted on the right y-axis. The molar mass is plotted in black, while PMA and PSSA are plotted in pink and orange, respectively.

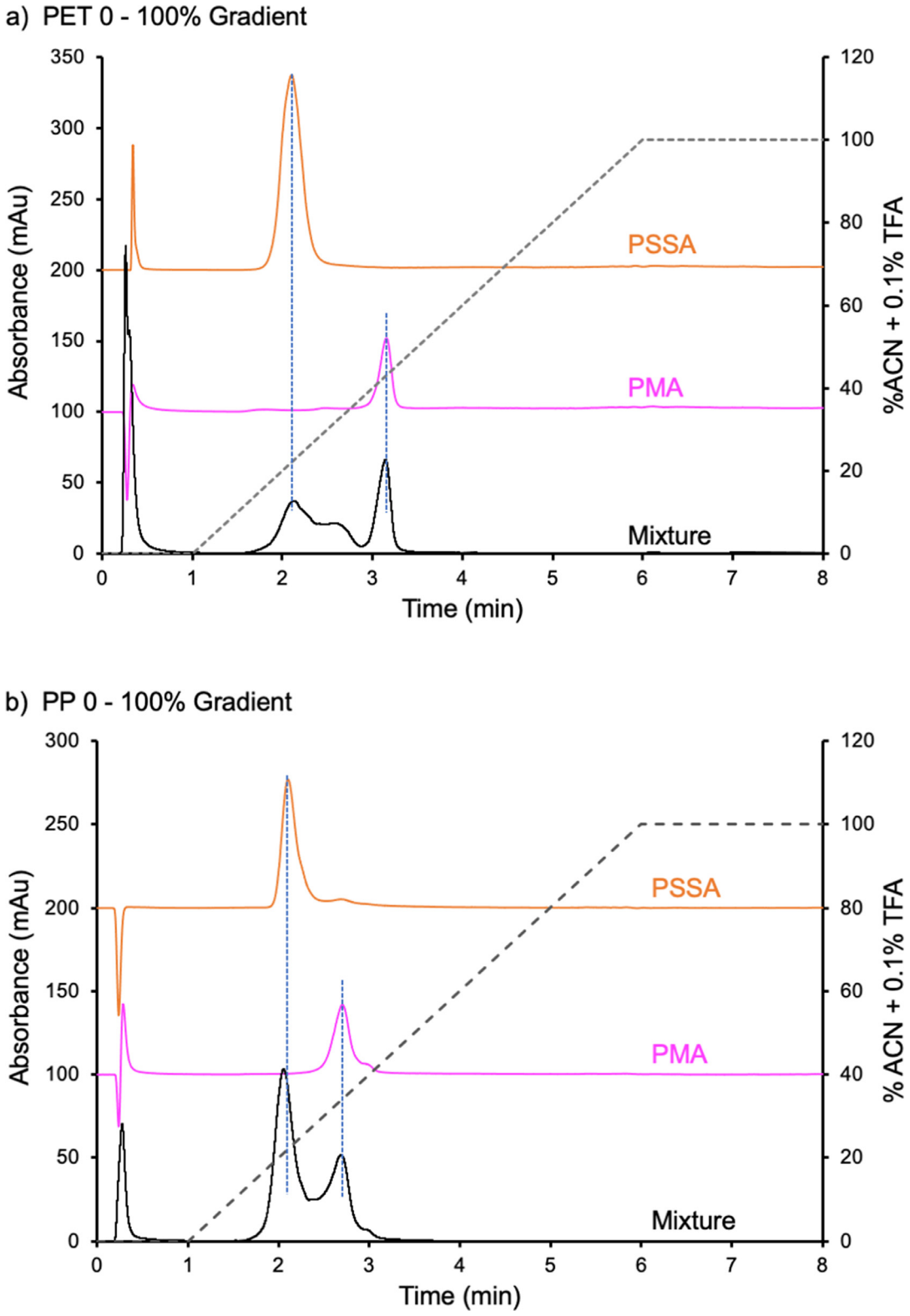

Fig. 4. RP separation of PMA and PSSA mixture on (a) PET and (b) PP C-CP fiber columns at flow rates of 0.5 mL min^{-1}. A 0 – 100% gradient was performed from DI + 0.1% TFA to ACN + 0.1% TFA, which is represented on the right y-axis.

PMA eluted later in the PET separations. As the two elution times are unexpected based on the lower hydrophobicity of the PET stationary phase (both would be expected to be shorter), additional forms of interaction between the polymer solutes and the stationary phase are indicated. Here, as noted in the previous protein separations comparing the PP and PET phases, it is clear that electrostatic interactions surelty play a role in the solute retention on PET [53]. Additionally, it is noted that both PET and PMA have carbonyl/carboxylate groups present, meaning hydrogen bonding interactions between the two could occur, with both entities be-

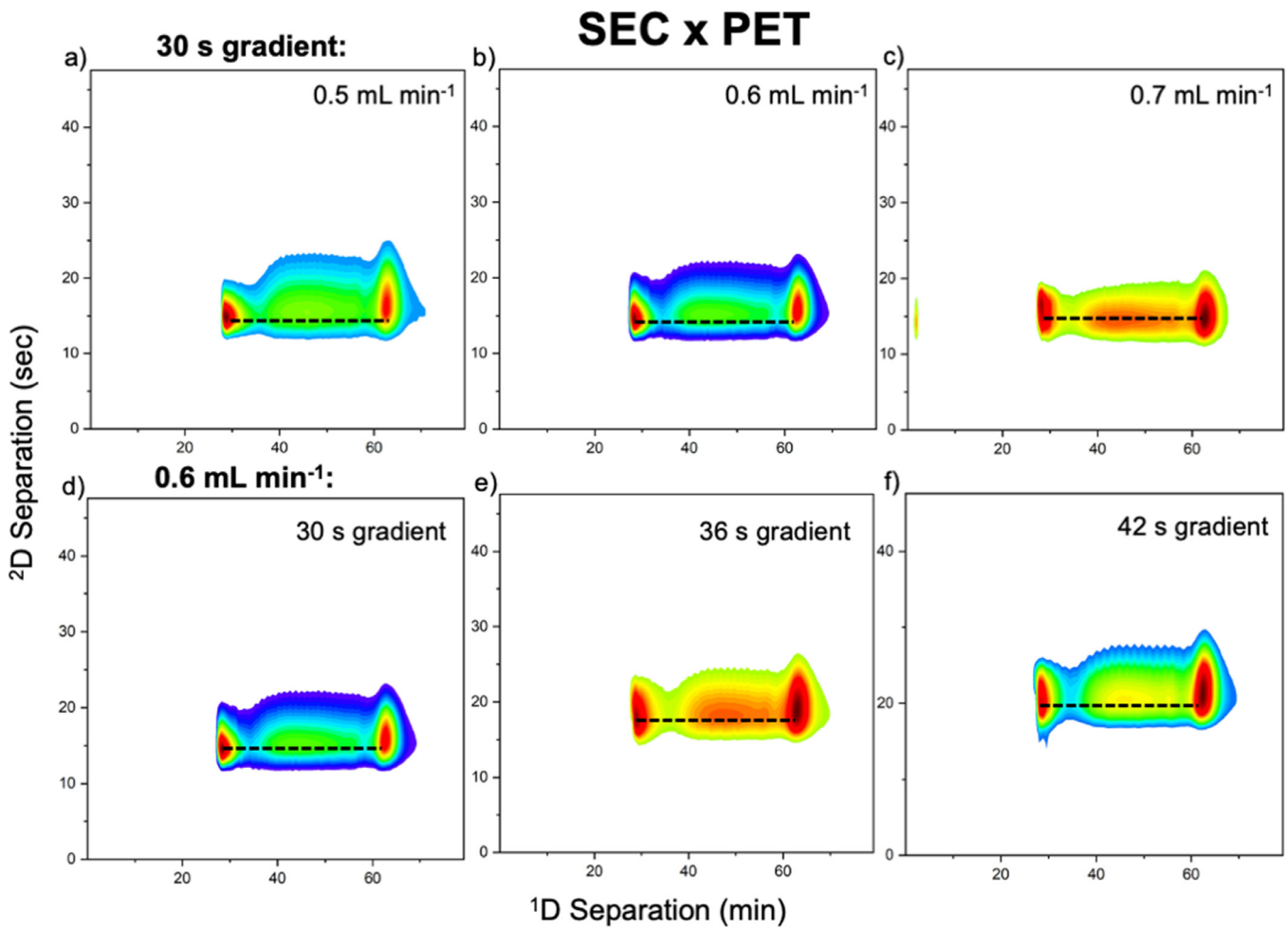

Fig. 5. SEC x PET separation optimizing the flow rate for the ^{2}D PET separation: (a) 0.5 mL min^{-1}, (b) 0.6 mL min^{-1}, and (c) 0.7 mL min^{-1} and the ^{2}D gradient time: (d) 30 s, (e) 36 s, and (f) 42 s. The ^{1}D SEC separation is represented on the x-axis, while the ^{2}D RP separation on the PET fiber column is represented on the y-axis. SEC separations were at 70:30 DI + 0.1% TFA: ACN + 0.1% TFA at a flow rate of 0.1 mL min^{-1}. The ^{2}D RP gradients were from 0 to 50% ACN + 0.1% TFA.

ing donors/acceptors. These interactions have been previously observed for these polymers, and have been found to become more prevalent at low pH [70]. The presence of an interaction between the two polymers, PMA and PSSA, is suggested in the separation of the mixture on the PET fiber stationary phase, with the response for PSSA altered, but the shape and recovery of PSSA being unaffected. The recovery of each polymer was determine based on the peak area of the individual injections versus the mixture to be ~ 95%, confirming little polymer is lost due to the interaction exhibited in the mixture. With the presence of the sulfonate groups and the carboxylate groups on the PSSA and PMA, respectively, interactions between these two groups can include hydrophilic, hydrogen bonding, and electrostatic interactions [71]. Indeed, the reduced and broadened response of the PSSA suggests the potential for two populations of the PSSA; one fraction adsorbed to the PET surface and the other perhaps co-adsorbed with PMA. Both of these populations elute prior to the critical mobile phase composition of PMA, thus it elutes unperturbed. It is important to note that the recoveries of both polymer species, based on the integrated peak areas, is not comprised in the mixture. This would seem to indicate that the fiber column itself is not suffering from overload effects or secondary (irreversible) chemical reactions.

The RP separation with the PP fiber stationary phase is shown in Fig. 4b, where PSSA is again seen to elute earlier in the gradient than PMA, predominately in a single band centered at a retention time of 2 min, with a very minor fraction eluting at ~2.6 min. PMA is more retained under RP conditions, with a primary band centered at ~2.7 min, with an unresolved trailing shoulder of approximately 20% relative absorbance. Here again, the elution of the PMA occurs at a lower percentage-B than for the PET phase (Fig. 4a), suggestive of other forms of interaction in that case, such as pi-pi interactions or hydrogen bonding. The elution order of the two polymers on PP is as expected, as the sulfonic acid groups on the PSSA polymer have a more hydrophilic character than PMA [62]. At a low pH (e.g., 0.1% TFA), PMA is in a coiled conformation where the hydrophobic sites are more exposed [65–69]. Very different from the situation observed in the SEC chromatograms of the mixtures (Fig. 2), the RP chromatogram of the mixture here bears little difference from a linear combination of the two-component polymers, suggesting little to no interaction between the two solutes. Again the recovery of the polymers was determined to be ~109%, indicating the polymer is fully eluted and not affected by the mixture. The increase in the recovery can be due to the error in the manual injections or the dilution of the sample. Additionally, the observed diversity in molecular weight-space (i.e. the SEC chromatograms) is not apparent in the RP-space, suggesting that the enthalpic interactions across the populations of each polymer type are fairly monodispersed. The ability to affect different levels of chemical selectivity, even when using the same RP gradients, is seen as an added level of chemical information which can be obtained using the multiple C-CP fiber phases; PET being moderately hydrophobic with higher-order interactions being pos-

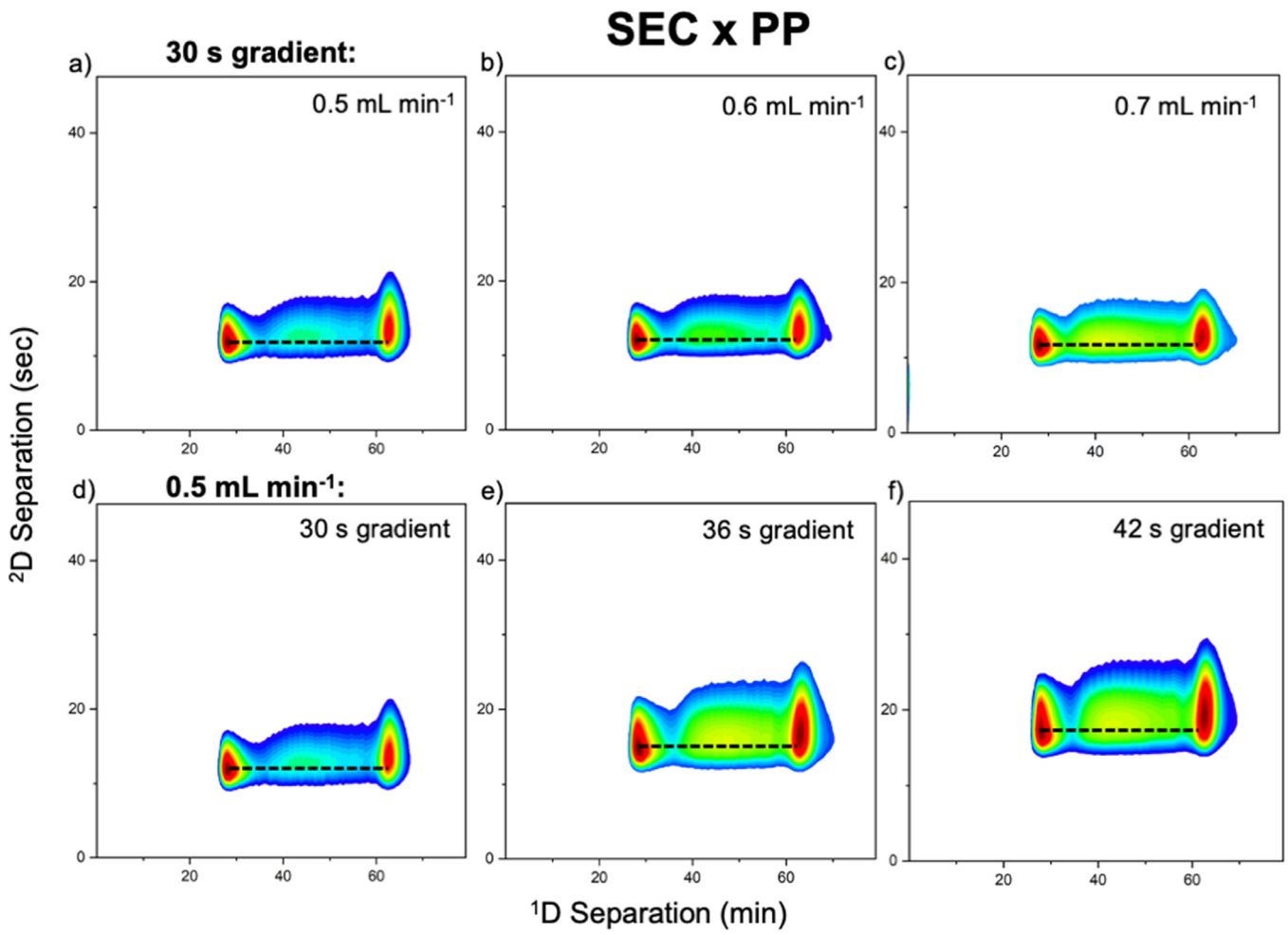

Fig. 6. SEC x PP separation optimizing the flow rate: (a) 0.5 mL min^{-1}, (b) 0.6 mL min^{-1}, and (c) 0.7 mL min^{-1} and the ^{2}D gradient time: (d) 30 s, (e) 36 s, and (f) 42 s. The ^{1}D SEC separation is represented on the x-axis, while the ^{2}D RP separation on the PP fiber column is represented on the y-axis. SEC separations were at 70:30 DI + 0.1% TFA: ACN + 0.1% TFA at a flow rate of 0.1 mL min^{-1}. The ^{2}D RP gradients were from 0 to 50% ACN + 0.1% TFA.

sible and PP which is very hydrophobic and otherwise chemically inactive.

3.2. ^{2}D separations

3.2.1. SEC x RP

Ideally, two-dimensional separations encompass two orthogonal separation modalities, with compatible solvents, to achieve the optimum peak capacity. The two separation modalities for this 2DLC coupling include SEC and RP, implemented as SEC x RP and RP x RP. RP was solely used in the ^{2}D due to the fast separation capability of the C-CP fiber columns and the added potential for mass spectrometric detection if desired. (If SEC implementation is needed in ^{2}D, a short SEC column or elevated temperature would be required, leading to poor resolution and potential column degradation, respectively.) The first coupling placed SEC in the ^{1}D and RP in the ^{2}D. Both PET and PP fiber columns were employed in the ^{2}D. The mobile phase flow rate and ^{2}D gradient times were varied to determine optimal separation conditions. Flow rates were varied from 0.5 to 0.7 mL min^{-1} and the ^{2}D gradient times varied from 30 to 42 s.

The type of gradient used in the ^{2}D, including full and shift gradients, affects the observed resolution. While shift gradients are commonly used due to the short range of MP covered in each transfer, confounding wraparound behavior can be observed, where strongly retained species are not fully eluted in the transferred fraction. With the SEC placement in the ^{1}D, which is solely based on the hydrodynamic volume, a shift gradient for the ^{2}D could be ill-representative of the composition. Specifically, small, slightly hydrophobic species will elute later in the ^{1}D, and will therefore be unretained in the ^{2}D as the MP has already shifted to a higher organic composition (i.e., solutes may elute in the ^{2}D injection volume). The use of a full gradient (i.e., same gradient with each transfer) in this case would be more representative as it covers the same MP range for each successive transfer.

The product chromatograms corresponding to variations in ^{2}D flow rate and gradient times for the SEC × PET and SEC × PP separations are shown in Figs. 5 and 6, respectively. For both 2DLC separations, the ^{1}D SEC separation conditions correspond to the standalone (1D) separation shown in Fig. 2d, employing a 30% ACN mobile phase, but at a flow rate reduced to 0.1 mL min^{-1} for more comprehensive sampling into ^{2}D. For the SEC x PET coupling (Fig. 5) the flow rate was first varied from 0.5 to 0.7 mL min^{-1} with a 30 s gradient time. (Dashed line in the chromatograms is added to aid the eye in regards to 2D elution times.) The chromatograms each show two distinct bands, with a fairly diffuse band in between the two, as would be expected from the SEC chromatograms of Fig. 2. In general, increases in flow rate in C-CP fiber macromolecule separations yield better resolution due to peak compression at the higher linear velocities [41,50,55]. In addition, solutes tend to elute at lower amounts of %B. At 0.5 mL min^{-1}, a differentiation between the two solutes in the ^{2}D elu-

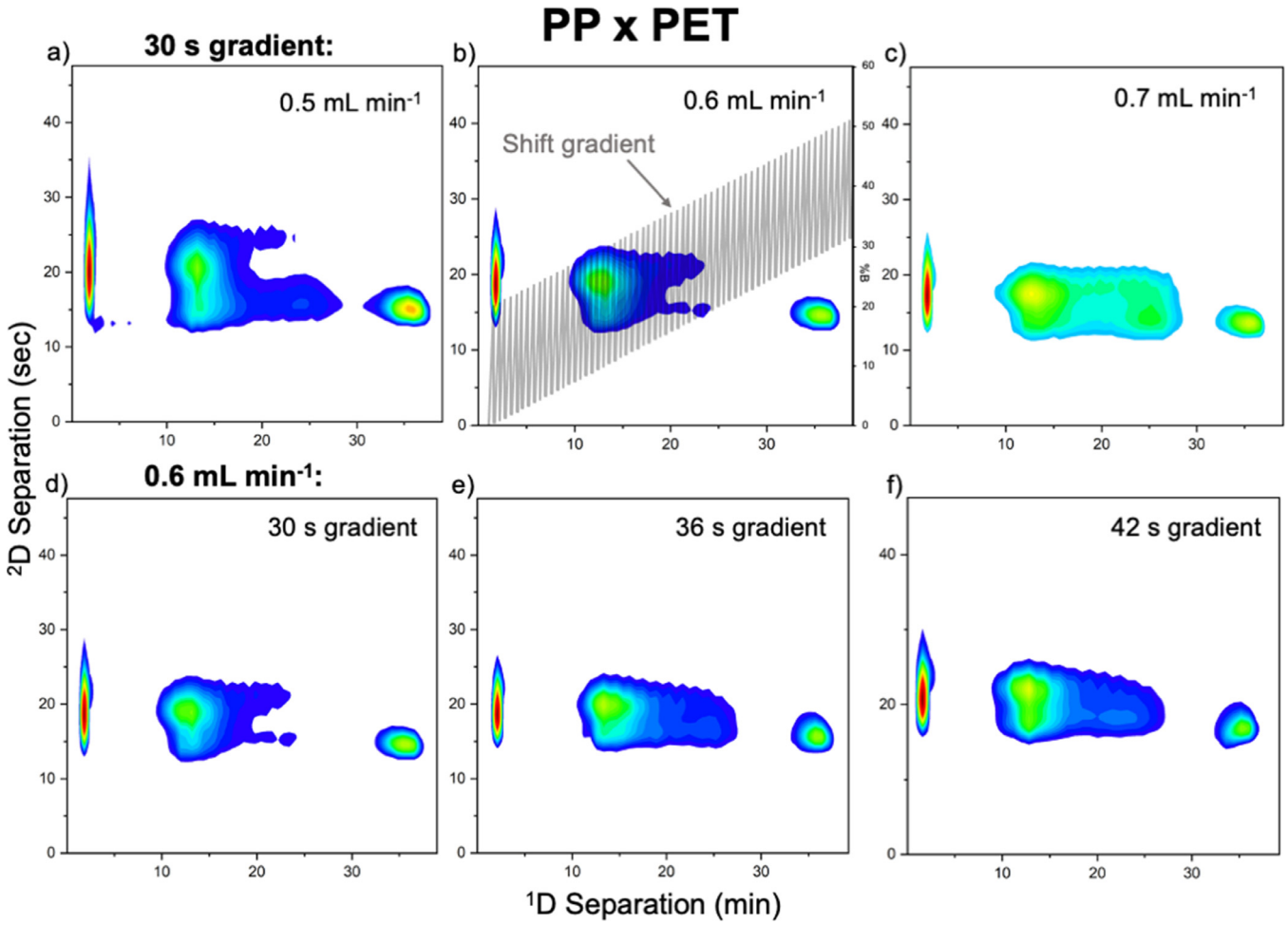

Fig. 7. PP x PET separation optimizing the flow rate: (a) 0.5 mL min^{-1}, (b) 0.6 mL min^{-1}, and (c) 0.7 mL min^{-1} and the ^{2}D gradient time: (d) 30 s, (e) 36 s, and (f) 42 s. The ^{1}D RP separation on the PP fiber column is represented on the x-axis, while the ^{2}D RP separation on the PET fiber column is represented on the y-axis. The ^{1}D PP separation was at a flow rate of 0.1 mL min and the gradient was from 0 to 50% ACN + 0.1% TFA. A shift gradient from 0 to 50% ACN + 0.1% TFA was used for the ^{2}D PET separation, as shown in black on the graph representing the 0.6 mL min^{-1} flow rate, with the %B on the right axis.

tion times is seen. Consistent with the much slower RP gradient 1D separation of Fig. 4a, the two solutes are seen here to elute with an approximately 10%B difference following the SEC separation. As the flow rate was increased to 0.6 mL min^{-1} and 0.7 mL min^{-1}, the differentiation in the ^{2}D elution times is somewhat diminished, though the elution bandwidths become more concentrated (lower total breadth), as expected. The higher flow rate appears to provide greater recovery of the PSSA fraction across the ^{1}D elution time, though no quantitative conclusions can be made due to the differing extents of background absorbance correction. Interestingly, across each of the experimental conditions of the SEC x RP couplings, the interband region has 2D elution characteristics that follow those of PSSA, reinforcing the assumption that this band represented a form of that solute. To further evaluate the separation in ^{2}D, the gradient times were adjusted from 30 to 42 s at a constant flow rate of 0.6 mL min^{-1}; followed by a 6 s re-equilibration step in each case. It is important to consider the entirety of ^{2}D separation time (gradient + re-equilibration) as this is the time that the injection loop is filling with ^{1}D eluate, with values between 20 and 80% fill being the target based on manufacturer recommendations. Based on the 0.5 mL min^{-1} flow rate, the injector becomes 75% full at the shortest gradient time, increasing to 100% at the longest gradient time. Indeed, the longer two gradient times are likely to be susceptible to overfill losses. This added filling is evidenced in the greater responses in the interband elution regions, with no appreciable gains in the latter case. More importantly, the width of the elution bands (in ^{2}D time-space) shows a time-stagger and some band broadening, as expected as the elutes cover the same gradient percentages over longer times. As such, the 30 s 2D gradient time was deemed optimal for the SEC x PET separation case.

For the SEC x PP separation, similar chromatograms are observed (Fig. 6) to the SEC x PET case, with the two primary bands and the diffuse one in between. Again, the flow rates were varied from 0.5 to 0.7 mL min^{-1} with a 30 s gradient, revealing sharper peaks with higher flow rates but losing the retention time differentiation between the solutes in the second dimension. While operation at 0.7 mL min^{-1} appears to again provide greater recoveries, the loss of ^{2}D differentiation could be problematic. In this case, the 0.6 mL min^{-1} was deemed to be optimal as lesser band broadening was present versus 0.5 mL min^{-1}, but differentiation between solutes was still observed. As before, with the variations in gradient time in the ^{2}D (30 – 42 s), there was significant broadening, sample loss, and no improvement in second dimension resolution provided by increasing the time. In comparison to the SEC x PET separations (Fig. 5), there is little differentiation, except for the slightly later elution time (~3–6 s) in ^{2}D when the PET is used, reflective of the greater retention of the PMA species. Overall for the SEC x RP separations, the SEC provides resolution in terms of hydrodynamic sizing, however, little enhanced differentiation is observed between the two polymer types in the RP separation; i.e.,

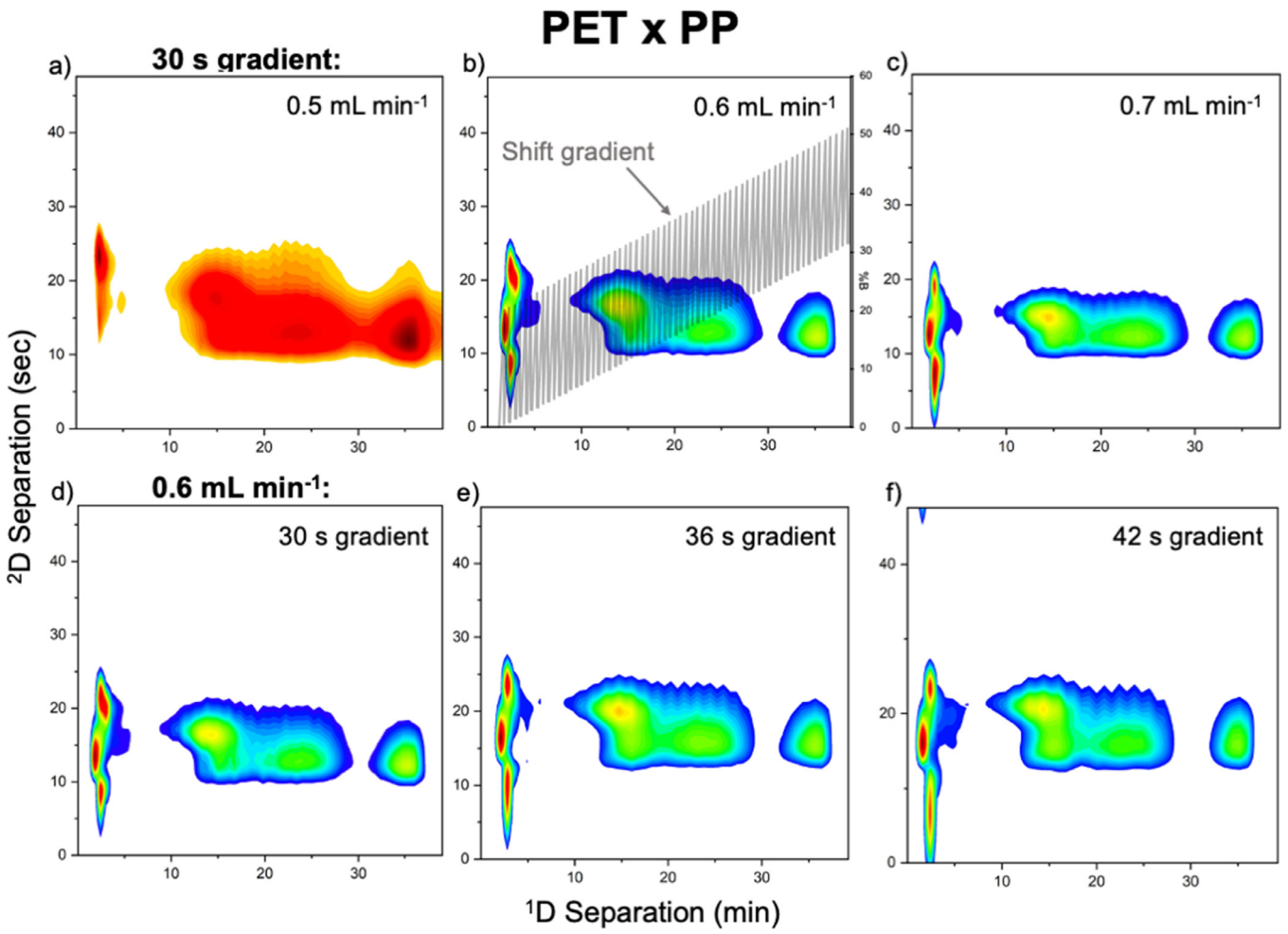

Fig. 8. PET x PP separation optimizing the flow rate: (a) 0.5 mL min^{-1}, (b) 0.6 mL min^{-1}, and (c) 0.7 mL min^{-1} and the ^{2}D gradient time: (d) 30 s, (e) 36 s, and (f) 42 s. The ^{1}D RP separation on the PET fiber column is represented on the x-axis, while the ^{2}D RP separation on the PP fiber column is represented on the y-axis. The ^{1}D PET separation was at a flow rate of 0.1 mL min and the gradient was from 0 to 50% ACN + 0.1% TFA. A shift gradient from 0 to 50% ACN + 0.1% TFA was used for the ^{2}D PP separation, as shown in black on the graph representing the 0.6 mL min^{-1} flow rate, with the %B on the right axis.

little added information in the second dimension. That said, direct coupling to ESI-MS could be a strong asset for the approach.

3.2.2. RP x RP

While the respective polymer solutes elute in close proximity in the 1D RP separations on each of the fiber phases (Fig. 4), the absolute elution solvent strengths are different between the PP and PET phases. While not quite orthogonal, the two different RP phases do provide a level of differentiation. The RP x RP separation strategy provides two potential practical advantages over SEC x RP in terms of reduced analysis times and the abilty to operate in more dilute solutions or lower injection volumes due to lesser dilution in the first dimension versus SEC. PET and PP fibers were used in both dimensions, with the ^{2}D flow rates (0.5 mL min^{-1} – 0.7 mL min^{-1}) and gradient times (30 – 42 s) similarly varied. Initially, the same concentration of polymer sample was used for the RP x RP separation but was diluted to lower concentrations (0.595 mg mL^{-1} PMA and 0.05 mg mL^{-1} of PSSA) because less dilution occurs during the separation with the C-CP fiber columns versus SEC. A shift gradient was used in the RP × RP, where the starting mobile phase composition of ^{2}D "shifts" to follow the mobile phase composition of the ^{1}D (as superimposed in the figures). More specifically, the eluate is introduced into a complementary MP composition in the ^{2}D separation. The RP × RP separation provides a probe to the hydrophobic (and perhaps higher order) interaction sites, allowing evaluation of the chemical heterogeneity of the respective polymer solutes.

The chromatograms of the PP x PET separations are shown in Fig. 7, with the flow rates and separation times varied as the previous SEC x RP separations (Figs. 5 and 6). A gradient from 0 to 50% was used for the ^{1}D RP separation, where two distinct regions, corresponding to the %B compositions of relevance found in the 1D RP separations of Fig. 4a. While two pronounced bands are seen, corresponding to PSSA and PMA, clearly seen in this case is a narrow band of virtually-unretained species eluting from ^{1}D to ^{2}D. Indeed, that species is infact retained on the second dimension, eluting in the normal course of the gradient. It may be assumed that these eluates are low molecular weight polar molecules, likely monomers of one of the primary polymers. The pronounced tailing observed for the primary PSSA peak (~11 min) is consistent with Fig. 4a, but is cleanly resolved from the PMA in this case. In fact, with the ^{2}D RP separation added, there is a distinct level chemical heterogeneity observed for the PSSA, with the main PSSA species exhibiting a broad range in hydrophobicity eluting from ~13 to 27 s, while the tail exhibits shows far less range eluting ~14 – 20 s. The large elution range is likely revealing a range of sulfonated end groups present on the polymer. A previous study observed how the degree of sulfonation affects the hydrophobicity of a compound, specifically that more sulfonic acid groups decrease the hydrophobic character [62], which is supported by eluting at lower percent-

ages of ACN. The large elution span can therefore be linked to a large degree of variability in sulfonation present within the PSSA. Additionally, not seen in the 1D space, there appears to be a small, discrete PSSA population that elutes in between the primary PSSA and PMA peaks. The PMA elution shows little polydispersity as one uniform peak eluting over a small range of organic solvent compositions in both dimensions. This high %B elution would appear to correspond to the coiled conformation of PMA with high hydrophobic character as cited in literature [65–69]. Increases in the ^{2}D flow rates (at the same 30 s gradient time) result in the expected, more narrow elution bands in the second dimension, In doing so, the secondary PSSA band becomes more well-defined, though the percentage-B differences between the two polymers are reduced. Choosing the ^{2}D mobile phase flow rate of 0.6 mL min^{-1} as be optimal, the ^{2}D gradient time was varied from 30 to 42 s. As in the case of using PET in the second dimension of SEC X RP, use of the fastest gradient provides more narrow ^{2}D elution bands, while also minimizing the possibilities of sample loss due to overfilling of the injector as exhibited in the broadening of the PSSA band in the first dimension.

Subsequently, the PET x PP fiber columns were coupled, where the more hydrophobic stationary phase is in ^{2}D, with chromatograms shown in Fig. 8. Recent studies with derivatized silica phases have shown that incorporating the more hydrophobic column in ^{2}D improves elution bandwidth suppression (i.e., better resolution) [72,73]. The more hydrophobic stationary phase in this case, the PP fibers in ^{2}D, exhibited retention of the species that were unretained on the PET column in the ^{1}D. Seen are three separate species that are differentiated due to the more hydrophobic nature of PP, rather than the single band present in the injection/void volume in the PP x PET coupling (Fig. 7). These species could be small molecule impurities in the polymer mixture or a discrete population of monomeric species having little hydrophobic character. (Fortuitously, while the separation speed in the second RP separation is too rapid for MALS analysis, these species could be readily identified via coupling with ESI-MS.) For the PET x PP separation, there are three regions present, which are also present in the ^{1}D PET separation in Fig. 4a; PSSA, an apparent PSSA-PMA complex, and the PMA eluting with little polydispersity present. As shown in the PP x PET separation (Fig. 7), the main PSSA peak shows a larger range in hydrophobicity, eluting across ~10 – 22 s in ^{2}D for the 0.5 mL min^{-1} flow rate, while the shoulder exhibits slightly less of a range from ~10 to 19 s. With respect to the higher ^{2}D flow rates, the expected bandwidth suppression is seen, with the PSSA shoulder evolving into more of a distinct band for the 0.6 mL min^{-1} flow rate. Interesting as well, the range of hydrophobicities (^{2}D elution band widths) change across the overall population. Evaluation of the influence of gradient time in ^{2}D for the flow rate of 0.6 mL min^{-1} reveals further refinement in the polymer population profiles, with the intermediate gradient time (36 s, Fig. 8e) providing greater definition yet, suggesting three separate PSSA populations, two in the primary band and the co-polymer region. In fact, it becomes more clear in this case that all the three solutes appearing to elute in the ^{1}D injection void volume are actually not, with two of the solutes showing some amount of retention. That said, the longer gradients clearly suggest that the initial PSSA band itself is composed of two populations.

Overall, based on comparisons of the chromatograms presented in Figs. 5–8, there is a greater level species differentiation of the RP x RP scenario than SEC x RP; yielding 7 distinct species in the first case, and 3 in the latter. In the SEC x RP coupling, there is only differentiation based on the hydrodynamic volume of the polymer, with little added value beyond the potential use of ESI-MS detection following the RP stage. For the RP x RP separations, separation based on the hydrophobicity can be seen from both the x axis and y axis of the two dimensional plots.

4. Conclusions

C-CP fiber capillary columns were used in the 2D separation of two water-soluble polymers, PMA and PSSA. Orthogonality was achieved in two scenarios; SEC x RP separations with PET and PP used in ^{2}D (SEC x PET, SEC x PP) and RP x RP separations PET x PP and PP x PET couplings. The use of the fiber columns in ^{2}D eliminates the need for UPLC hardware in the second dimension. In and of itself, the SEC revealed and interesting chemistry that occurred between the two polymers, affecting the elution of the PSSA, but not the PMA. In-line MALS detection following SEC separations proved valuable for accessing the molecular weight of each polymer, revealing large differences versus the expected value. As a general rule, both of the SEC x RP couplings yielded little additional chemical information for this mixture, but would still be beneficial relative to the use of ESI-MS to identify the eluting species. The fiber-based RP x RP couplings provided far greater chemical information than the SEC x RP as a greater number of distinct species is revealed. Additionally, the fiber column RP x RP separations, shorter overall analysis times were achieved, along with lower concentrations of samples being required. These characteristics are a direct result of the physical structure of the fiber phases, where van Deemter C-terms are non-existent and recoveries are extremely high. While both phases can accommodate standard RP elution programs, they differ among themselves to an extent that clearly reveals greater numbers of solute populations in the chemistry of the polymers. That said, the diversity of C-CP fiber surface chemistries, both native and readily achieved through derivatization, opens up many avenues for their use in 2DLC. As a final consideration, it would be instructive to compare the fiber RP phases with commercial gigapore, aliphatically derivatized phases. Previous comparisons of this type in the realm of protein separations (up to MW = 650 kDA), showed clear hydrodynamic benefits of the fibers versus superficially porous and monolithic phases [52]. But surely, comparable 2D studies of these sorts of water- soluble polymers are in order.

Declaration of Competing Interest

The authors have no financial conflict of interest to report.

CRediT authorship contribution statement

Sarah K. Wysor: Methodology, Data curation, Visualization, Writing – original draft. **R. Kenneth Marcus:** Conceptualization, Supervision, Writing – review & editing.

Data availability

Data will be made available on request.

Acknowledgments

This project was supported in part by National Science Foundation grant CHE-2107882.

References

[1] D.Q.M. Craig, The mechanisms of drug release from solid dispersions in water–soluble polymers, Int. J. Pharm. 231 (2) (2002) 131–144.
[2] V.G. Kadajji, G.V. Betageri, Water soluble polymers for pharmaceutical applications, Polymers 3 (4) (2011) 1972–2009.
[3] T. Tagami, N. Hayashi, N. Sakai, T. Ozeki, 3D printing of unique water-soluble polymer-based suppository shell for controlled drug release, Int. J. Pharm. 568 (2019) 118494.
[4] N.K. Vasiliev, A.D.C. Pronk, I.N. Shatalina, F.H.M.E. Janssen, R.W.G. Houben, A review on the development of reinforced ice for use as a building material in cold regions, Cold Reg. Sci. Technol. 115 (2015) 56–63.

[5] P. Kilz, W. Radke, Application of two-dimensional chromatography to the characterization of macromolecules and biomacromolecules, Anal. Bioanal. Chem. 407 (1) (2015) 193–215.
[6] W.F. Su, Polymer size and polymer solutions, in: Principles of Polymer Design and Synthesis, Springer Berlin Heidelberg, Berlin, Heidelberg, 2013, pp. 9–26, doi:10.1007/978-3-642-38730-2_2.
[7] R. Xu, Light scattering: a review of particle characterization applications, Particuology 18 (2015) 11–21.
[8] L. Bokobza, Spectroscopic techniques for the characterization of polymer nanocomposites: a review, Polymers 10 (1) (2018) 7.
[9] M. Gaborieau, P. Castignolles, Size-exclusion chromatography (SEC) of branched polymers and polysaccharides, Anal. Bioanal. Chem. 399 (4) (2011) 1413–1423.
[10] D. Berek, Size exclusion chromatography – A blessing and a curse of science and technology of synthetic polymers, J. Sep. Sci. 33 (3) (2010) 315–335.
[11] W. Radke, A.H.E. Müller, Synthesis and characterization of comb-shaped polymers by SEC with on-line light scattering and viscometry detection, Macromolecules 38 (9) (2005) 3949–3960.
[12] Z. PENG, P.G. ILAND, A. OBERHOLSTER, M.A. SEFTON, E.J. WATERS, Analysis of pigmented polymers in red wine by reverse phase HPLC, Aust. J. Grape Wine Res. 8 (1) (2002) 70–75.
[13] K.J. Hilbert, R.K. Marcus, Separation of water-soluble polymers using capillary-channeled polymer fiber stationary phases, J. Sep. Sci. 33 (22) (2010) 3571–3577.
[14] P. Jandera, J. Fischer, H. Lahovská, K. Novotná, P. Česla, L. Kolářová, Two-dimensional liquid chromatography normal-phase and reversed-phase separation of (co)oligomers, J. Chromatogr. A 1119 (1) (2006) 3–10.
[15] J. Engelke, J. Brandt, C. Barner-Kowollik, A. Lederer, Strengths and limitations of size exclusion chromatography for investigating single chain folding – current status and future perspectives, Polym. Chem. 10 (25) (2019) 3410–3425 -UK.
[16] S. Neupane, K.S. Bittkau, S. Alban, Size distribution and chain conformation of six different fucoidans using size-exclusion chromatography with multiple detection, J. Chromatogr. A 1612 (2020) 460658.
[17] G. Brusotti, E. Calleri, R. Colombo, G. Massolini, F. Rinaldi, C. Temporini, Advances on size exclusion chromatography and applications on the analysis of protein biopharmaceuticals and protein aggregates: a mini review, Chromatographia 81 (1) (2018) 3–23.
[18] E.S.P. Bouvier, S.M. Koza, Advances in size-exclusion separations of proteins and polymers by UHPLC, TrAC Trends Anal. Chem. 63 (2014) 85–94.
[19] G. Meira, M. Netopilík, M. Potschka, I. Schnöll-Bitai, J. Vega, Band broadening function in size exclusion chromatography of polymers: review of some recent developments, Macromol. Symp. 258 (1) (2007) 186–197.
[20] R. Brighenti, Y. Li, F.J. Vernerey, Smart polymers for advanced applications: a mechanical perspective review, Front. Mater. 7 (2020).
[21] D. Li, C. Jakob, O. Schmitz, Practical considerations in comprehensive two-dimensional liquid chromatography systems (LCxLC) with reversed-phases in both dimensions, Anal. Bioanal. Chem. 407 (1) (2015) 153–167.
[22] S.E. Reichenbach, X. Tian, Q. Tao, D.R. Stoll, P.W. Carr, Comprehensive feature analysis for sample classification with comprehensive two-dimensional LC, J. Sep. Sci. 33 (10) (2010) 1365–1374.
[23] A. van der Horst, P.J. Schoenmakers, Comprehensive two-dimensional liquid chromatography of polymers, J. Chromatogr. A 1000 (1) (2003) 693–709.
[24] X. Jiang, A. van der Horst, V. Lima, P.J. Schoenmakers, Comprehensive two-dimensional liquid chromatography for the characterization of functional acrylate polymers, J. Chromatogr. A 1076 (1) (2005) 51–61.
[25] J.M. Davis, Dependence of effective peak capacity in comprehensive two-dimensional separations on the distribution of peak capacity between the two dimensions, Anal. Chem. 80 (21) (2008) 8122–8134.
[26] D.R. Stoll, X. Li, X. Wang, P.W. Carr, S.E. Porter, S.C. Rutan, Fast, comprehensive two-dimensional liquid chromatography, J. Chromatogr. A 1168 (1–2) (2007) 3–43 discussion 2.
[27] B.W.J. Pirok, D.R. Stoll, P.J. Schoenmakers, Recent developments in two-dimensional liquid chromatography: fundamental improvements for practical applications, Anal. Chem. 91 (1) (2019) 240–263.
[28] J.C. Giddings, Two-dimensional separations: concept and promise, Anal. Chem. 56 (12) (1984) 1258A–1270A.
[29] M.J. Gray, G.R. Dennis, P.J. Slonecker, R.A. Shalliker, Comprehensive two-dimensional separations of complex mixtures using reversed-phase reversed-phase liquid chromatography, J. Chromatogr. A 1041 (1) (2004) 101–110.
[30] Z. Liu, D.G. Patterson, M.L. Lee, Geometric approach to factor analysis for the estimation of orthogonality and practical peak capacity in comprehensive two-dimensional separations, Anal. Chem. 67 (21) (1995) 3840–3845.
[31] P.J. Slonecker, X. Li, T.H. Ridgway, J.G. Dorsey, Informational orthogonality of two-dimensional chromatographic separations, Anal. Chem. 68 (4) (1996) 682–689.
[32] S.C. Rutan, J.M. Davis, P.W. Carr, Fractional coverage metrics based on ecological home range for calculation of the effective peak capacity in comprehensive two-dimensional separations, J. Chromatogr. A 1255 (2012) 267–276.
[33] R.E. Murphy, M.R. Schure, J.P. Foley, Effect of sampling rate on resolution in comprehensive two-dimensional liquid chromatography, Anal. Chem. 70 (8) (1998) 1585–1594.
[34] P. Yang, W. Gao, J.E. Shulman, Y. Chen, Separation and identification of polymeric dispersants in detergents by two-dimensional liquid chromatography, J. Chromatogr. A 1566 (2018) 111–117.
[35] H.C. van de Ven, J. Purmova, G. Groeneveld, T.S. Bos, A.F.G. Gargano, S. van der Wal, Y. Mengerink, P.J. Schoenmakers, Living with breakthrough: two-dimensional liquid-chromatography separations of a water-soluble synthetically grafted bio-polymer, Separations 7 (3) (2020) 41.
[36] P. Kilz, Two-dimensional chromatography as an essential means for understanding macromolecular structure, Chromatographia 59 (1) (2004) 3–14.
[37] R.K. Marcus, W.C. Davis, B.C. Knippel, L. LaMotte, T.A. Hill, D. Perahia, J.D. Jenkins, Capillary-channeled polymer fibers as stationary phases in liquid chromatography separations, J. Chromatogr. A 986 (1) (2003) 17–31.
[38] R.D. Stanelle, C.A. Straut, R.K. Marcus, Nylon-6 capillary-channeled polymer fibers as a stationary phase for the mixed-mode ion exchange/reversed-phase chromatography separation of proteins, J. Chromatogr. Sci. 45 (7) (2007) 415–421.
[39] R.D. Stanelle, L.C. Sander, R.K. Marcus, Hydrodynamic flow in capillary-channel fiber columns for liquid chromatography, J. Chromatogr. A 1100 (1) (2005) 68–75.
[40] D.K. Nelson, R.K. Marcus, A novel stationary phase: capillary-channeled polymer (C-CP) fibers for HPLC separations of proteins, J. Chromatogr. Sci. 41 (9) (2003) 475–479.
[41] J.M. Randunu, R.K. Marcus, Microbore polypropylene capillary channeled polymer (C-CP) fiber columns for rapid reversed phase HPLC of proteins, Anal. Bioanal. Chem. 404 (2012) 721–729.
[42] L. Wang, R.K. Marcus, Evaluation of protein separations based on hydrophobic interaction chromatography using polyethylene terephthalate capillary-channeled polymer (C-CP) fiber phases, J. Chromatogr. A 1585 (2019) 161–171.
[43] L. Jiang, R.K. Marcus, Microwave-assisted, grafting polymerization preparation of strong cation exchange nylon 6 capillary-channeled polymer fibers and their chromatographic properties, Anal. Chim. Acta 977 (2017) 52–64.
[44] L. Jiang, R.K. Marcus, Microwave-assisted grafting polymerization modification of nylon 6 capillary-channeled polymer fibers for enhanced weak cation exchange protein separations, Anal. Chim. Acta 954 (2017) 129–139.
[45] L. Jiang, Y. Jin, R.K. Marcus, Polyethylenimine modified poly(ethylene terephthalate) capillary channeled-polymer fibers for anion exchange chromatography of proteins, J. Chromatogr. A 1410 (2015) 200–209.
[46] H.K. Trang, A.J. Schadock-Hewitt, L. Jiang, R.K. Marcus, Evaluation of loading characteristics and IgG binding performance of Staphylococcal protein A on polypropylene capillary-channeled polymer fibers, J. Chromatogr. B (2016) 92–104 1015-1016.
[47] H.K. Trang, R.K. Marcus, Application of protein A-modified capillary-channeled polymer polypropylene fibers to the quantitation of IgG in complex matrices, J. Pharm. Biomed. Anal. 142 (2017) 49–58.
[48] A.J. Schadock-Hewitt, R.K. Marcus, Initial evaluation of protein A modified capillary-channeled polymer fibers for the capture and recovery of immunoglobulin G, J. Sep. Sci. 37 (5) (2014) 495–504.
[49] L. Wang, H.K. Trang, J. Desai, Z.D. Dunn, D.D. Richardson, R.K. Marcus, Fiber-based HIC capture loop for coupling of protein A and size exclusion chromatography in a two-dimensional separation of monoclonal antibodies, Anal. Chim. Acta 1098 (2020) 190–200.
[50] D.M. Nelson, R.K. Marcus, Potential for ultrafast protein separations with capillary-channeled polymer (C-CP) fiber columns, Protein Pept. Lett. 13 (1) (2006) 95–99.
[51] L. Wang, R.K. Marcus, Polypropylene capillary-channeled polymer fiber column as the second dimension in a comprehensive two-dimensional RP X RP analysis of a mixture of intact proteins, Anal. Bioanal. Chem. 412 (2020) 2963–2979.
[52] L.S. Billotto, R.K. Marcus, Comparative analysis of trilobal capillary-channeled polymer fiber columns with superficially porous and monolithic phases towards reversed-phase protein separations, J. Sep. Sci. 45 (2022) 3811–3826.
[53] D.K. Nelson, R.K. Marcus, Characterization of capillary-channeled polymer (C-CP) fiber stationary phases for high-performance liquid chromatography protein separations: comparative analysis with a packed-bed column, Anal. Chem. 78 (2006) 8462–8471.
[54] Z. Wang, R.K. Marcus, Determination of pore size distributions in capillary-channeled polymer fiber stationary phases by inverse size exclusion chromatography (iSEC) and implications for fast protein separations, J. Chromatogr. A 1351 (2014) 82–89.
[55] K.M. Randunu, S. Dimartino, R.K. Marcus, Dynamic evaluation of polypropylene capillary-channeled fibers as a stationary phase in high-performance liquid chromatography, J. Sep. Sci. 35 (23) (2012) 3270–3280.
[56] K.M. Randunu, R.K. Marcus, Microbore polypropylene capillary channeled polymer (C-CP) fiber columns for rapid reversed-phase HPLC of proteins, Anal. Bioanal. Chem. 404 (3) (2012) 721–729.
[57] D.R. Stoll, P.W. Carr, Two-dimensional liquid chromatography: a state of the art tutorial, Anal. Chem. 89 (1) (2017) 519–531.
[58] D.R. Stoll, Chapter 7 - introduction to two-dimensional liquid chromatography—theory and practice, in: M. Holčapek, W.C. Byrdwell (Eds.), Handbook of Advanced Chromatography/Mass Spectrometry Techniques, AOCS Press2017, pp. 227–286. 10.1016/B978-0-12-811732-3.00007-8.
[59] D. Berek, Two-dimensional liquid chromatography of synthetic polymers, Anal. Bioanal. Chem. 396 (1) (2010) 421–441.
[60] A. Baumgaertel, E. Altuntaş, U.S. Schubert, Recent developments in the detailed characterization of polymers by multidimensional chromatography, J. Chromatogr. A 1240 (2012) 1–20.
[61] S. Fekete, A. Beck, J.L. Veuthey, D. Guillarme, Theory and practice of size exclusion chromatography for the analysis of protein aggregates, J. Pharm. Biomed. Anal. 101 (2014) 161–173.
[62] L. Moreno Ostertag, X. Ling, K.F. Domke, S.H. Parekh, M. Valtiner, Characterizing the hydrophobic-to-hydrophilic transition of electrolyte structuring in pro-

ton exchange membrane mimicking surfaces, Phys. Chem. Chem. Phys. 20 (17) (2018) 11722–11729.
[63] J.E. Coughlin, A. Reisch, M.Z. Markarian, J.B. Schlenoff, Sulfonation of polystyrene: toward the "ideal" polyelectrolyte, J. Polym. Sci. A 51 (11) (2013) 2416–2424.
[64] R.C. Michel, W.F. Reed, New evidence of the nonequilibrium nature of the "slow modes" of diffusion in polyelectrolyte solutions, Biopolymers 53 (1) (2000) 19–39.
[65] D.F. Anghel, S. Saito, A. Iovescu, A. Băran, G. Stîngă, Counterion Effect of Cationic Surfactants Upon the Interaction with Poly(methacrylic acid), J. Surfactants Deterg. 14 (1) (2011) 91–101.
[66] D.Y. Chu, J.K. Thomas, Effect of cationic surfactants on the conformation transition of poly(methacrylic acid), J. Am. Chem. Soc. 108 (20) (1986) 6270–6276.
[67] J.J. Kiefer, P. Somasundaran, K.P. Ananthapadmanabhan, Interaction of tetradecyltrimethylammonium bromide with poly(acrylic acid) and poly(methacrylic acid). Effect of charge density, Langmuir 9 (5) (1993) 1187–1192.
[68] S. Saito, Properties of nonionic surfactant-polymethacrylic acid complexes: comparison with the polyacrylic acid complexes, J. Colloid Interface Sci. 165 (2) (1994) 505–511.
[69] H. Katsuura, H. Kawamura, M. Manabe, H. Kawasaki, H. Maeda, Binding of a surfactant counterion to low-charge-density poly(acrylic acid) and poly(methacrylic acid), Colloid Polym. Sci. 280 (1) (2002) 30–37.
[70] L. Sawyer, M.N.G. James, Carboxyl–carboxylate interactions in proteins, Nature 295 (5844) (1982) 79–80.
[71] S. Sakata, Y. Inoue, K. Ishihara, Quantitative evaluation of interaction force between functional groups in protein and polymer brush surfaces, Langmuir 30 (10) (2014) 2745–2751.
[72] F. Bedani, W.T. Kok, H.G. Janssen, Optimal gradient operation in comprehensive liquid chromatography× liquid chromatography systems with limited orthogonality, Anal. Chim. Acta 654 (1) (2009) 77–84.
[73] D. Li, O.J. Schmitz, Use of shift gradient in the second dimension to improve the separation space in comprehensive two-dimensional liquid chromatography, Anal. Bioanal. Chem. 405 (20) (2013) 6511–6517.